Open access • Journal Article • DOI:10.1109/LAWP.2015.2435891

Half-Mode Substrate-Integrated-Waveguide Cavity-Backed Slot Antenna on Cork Substrate — Source link

Olivier Caytan, Sam Lemey, Sam Agneessens, Dries Vande Ginste ...+4 more authors

Institutions: Ghent University, University of Beira Interior

Published on: 01 Jan 2016 - IEEE Antennas and Wireless Propagation Letters (IEEE)

Topics: Antenna efficiency, Antenna measurement, Slot antenna, Antenna factor and Coaxial antenna

Half-Mode Substrate-Integrated-Waveguide Cavity-Backed Slot Antenna on Cork Substrate

Olivier Caytan[1], Sam Lemey[1], Sam Agneessens[1], Dries Vande Ginste[1], *Senior Member, IEEE,* Piet Demeester[1], *Fellow, IEEE,* Caroline Loss[2,3], Rita Salvado[2], and Hendrik Rogier[1], *Senior Member, IEEE*

***Abstract*— A wideband half-mode substrate-integrated-waveguide cavity-backed slot antenna covering all Unlicensed National Information Infrastructure (U-NII) radio bands (5.15 GHz–5.85 GHz) is designed, fabricated and validated. By a half-mode implementation of a multi-moded cavity with non-resonant slot, a compact ultra-wideband antenna is obtained with very stable radiation characteristics, owing to the excellent antenna/platform isolation. Cork material is applied as antenna substrate, making the proposed antenna suitable for integration into floors or walls. In free-space conditions, an impedance bandwidth of 1.30 GHz (23.7 %), a radiation efficiency of 85 %, a front-to-back ratio of 15.0 dB and a maximum gain of 4.3 dBi at 5.50 GHz are measured. Performance is also validated when the antenna is deployed on various dielectric or conducting platforms and underneath different dielectric superstrates. Only the latter slightly detunes the antenna's impedance bandwidth. Yet, the complete frequency band of interest remains covered, owing to additional design margins incorporated in the requirements. Its compactness, unobtrusive integration potential and stable high performance in different environments make this antenna topology an ideal candidate for Internet of Things applications.**

Keywords*— *802.11ac Wi-Fi, Cork antenna substrate, Half-mode (HM) substrate-integrated-waveguide (SIW) cavity-backed slot antenna, Internet of Things (IoT), Unlicensed National Information Infrastructure (U-NII) radio bands.

I. Introduction

THE Internet and the next generation of wireless communications are currently converging towards the so-called Internet of Things (IoT). The far-reaching integration of everyday objects into the network is a key feature of this evolution. Antennas for IoT applications pose specific design challenges [1]. Currently, there is a need for low-cost and low-profile antennas that can be invisibly integrated into objects. Implementing the antenna directly in the object's material leads to a significant cost and area reduction since the readily available material and area of the object itself are reused to construct the antenna. Hence, novel materials should be considered as antenna substrates. Furthermore, an antenna topology with high isolation between the antenna and its environment is required. This minimizes detuning due to objects in the antenna's near field and offers stable high radiation efficiency in different environments. In addition, coverage of multiple frequency bands or wideband performance is necessary for demanding state-of-the-art wireless applications.

Substrate-Integrated-Waveguide (SIW) cavity-backed antenna topologies [2] [3] have already shown great potential in addressing these design challenges. These low-profile planar topologies allow for unobtrusive integration into floor and wall materials. Furthermore, SIW-based antennas provide a very high radiation efficiency and a good front-to-back ratio (FTBR) thanks to surface wave suppression, and a high isolation between the antenna and its environment owing to the antenna cavity that contains the fields. This makes them excellently suited for very low power and battery powered applications. Moreover, various bandwidth enhancement techniques for SIW cavity-backed antennas have already been studied [3].

This letter proposes the first wideband half-mode (HM) SIW cavity-backed slot antenna on a cork substrate. A half-mode implementation of a multi-moded cavity with non-resonant slot is applied to realize a compact antenna covering the $5.15\,\text{GHz}$–$5.85\,\text{GHz}$ frequency band. This frequency band contains all Unlicensed National Information Infrastructure (U-NII) radio bands [4], used by 802.11ac stations, and is referred to as the $5\,\text{GHz}$ Wi-Fi band. As cork is a common floor and wall material, the proposed low-profile antenna may unobtrusively be integrated into floors or walls. To the authors' knowledge, the only prior use of cork as substrate was in [5] for narrow-band radio-frequency identification (RFID) applications.

Section II outlines all design aspects of the HMSIW cavity-backed slot antenna. Its performance is validated in Section III by measurements in free-space and in realistic operating conditions, when objects cover or support the antenna.

II. Antenna topology, requirements and design

The antenna, shown in Fig. 1, is implemented on a $3\,\text{mm}$ thick cork substrate, by Amorim Cork Composites S.A. The cork substrate is a composite agglomerate, made of cork granules bound by polyurethane and has a density of $0.145\,\text{g/cm}^3$. The conducting top patch and bottom groundplane are patterned in copper-plated taffeta electrotextile (sheet resistance of $0.2\,\Omega$/sq), glued to the substrate by thermally activated adhesive sheets. The conducting layers are connected by brass eyelets (outer diameter $d = 4\,\text{mm}$) that are spaced close enough to minimize radiation loss ($d_x/d \leq 2$ and $d_y/d \leq 2$) [2]. Prior to the antenna design, the dielectric constant ϵ_r and loss tangent $\tan\delta$ of cork are determined at $5.50\,\text{GHz}$ using the resonator technique in [6]. As cork material is slightly inhomogeneous, due to its high porosity and

[1] IBCN/Electromagnetics Group, Dept. of Information Technology, Ghent University/iMinds, 9000 Ghent, Belgium (e-mail: olivier.caytan@intec.ugent.be).

[2] FibEnTech, Dept. of Textile Science and Technology, University of Beira Interior, 6201-001 Covilhã, Portugal.

[3] CAPES Foundation, Ministry of Education of Brazil, Brasília DF70040-20, Brazil.

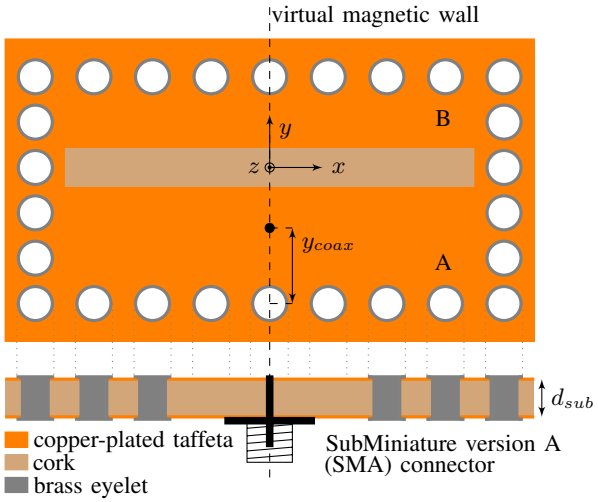

(a)

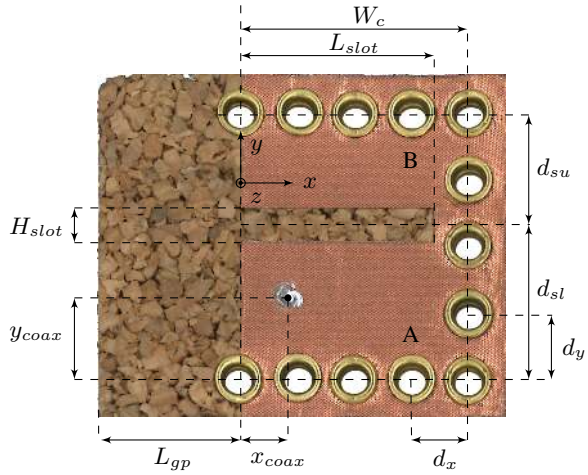

(b)

Fig. 1: (a) Substrate-integrated-waveguide (SIW) and (b) half-mode SIW cavity-backed slot antenna topology. Optimized dimensions: $d_{sub} = 3\,\text{mm}$, $W_c = 27.5\,\text{mm}$, $d_{su} = 13.5\,\text{mm}$, $d_{sl} = 18.4\,\text{mm}$, $H_{slot} = 4.1\,\text{mm}$, $L_{slot} = 23.5\,\text{mm}$, $x_{coax} = 5.0\,\text{mm}$, $y_{coax} = 9.5\,\text{mm}$, $L_{gp} = 15.0\,\text{mm}$, $d_x = 6.9\,\text{mm}$ and $d_y = 8.0\,\text{mm}$.

cellular structure, four resonators were characterized, yielding for $(\epsilon_r, \tan\delta)$: $(1.20, 0.0306)$, $(1.17, 0.0244)$, $(1.25, 0.0481)$ and $(1.26, 0.0421)$. In the design process, the average value $(1.22, 0.0363)$ is applied, while requiring robust antenna characteristics for varying cork material properties. This is achieved by adding impedance bandwidth margins that also compensate for antenna detuning. Specifically, we impose a $-10\,\text{dB}$ impedance bandwidth ranging from $4.85\,\text{GHz}$ to $6.15\,\text{GHz}$ to cover the $5\,\text{GHz}$ Wi-Fi band ($5.15\,\text{GHz}$–$5.85\,\text{GHz}$) with $300\,\text{MHz}$ margins.

To meet this requirement, a wideband multi-moded [7] SIW cavity-backed slot antenna topology is proposed. Fig. 1a shows the top conducting antenna patch and the vias that create the SIW cavity by connecting top patch and groundplane. A non-resonant slot in the top patch, much longer than half a wavelength, splits the cavity into parts A and B, leading to the simultaneous excitation of two hybrid cavity modes. The cavity and slot are dimensioned such that the resonance frequencies of the two excited hybrid modes are close together in the frequency band of interest, enlarging the impedance bandwidth. The hybrid mode with lower resonance frequency combines a strong TE_{120} with a weak TE_{110} mode. The fields in cavity parts A and B are out of phase, being dominant in part A. The hybrid mode with higher resonance frequency combines a strong TE_{110} with a weak TE_{120} mode. The fields in cavity parts A and B are in phase, being dominant in part B. Both hybrid modes radiate through the slot. A coaxial probe feed efficiently magnetically couples to the two hybrid modes and achieves a higher FTBR (being the ratio of the gain in the $+z$ direction to the gain in the $-z$ direction), compared to a grounded coplanar waveguide feed [7].

Being combinations of the TE_{110} and the TE_{120} modes, both hybrid modes exhibit a virtual magnetic wall coinciding with the YZ-plane. Hence, the top patch may be cut in half, removing the part for $x < 0$ together with the vias in that region, yielding the half-mode [8] implementation in Fig. 1b. Cavity width W_c clearly influences the resonance frequencies of both hybrid modes, with a wider cavity increasing the bandwidth. The length of cavity part A, d_{sl}, primarily affects the resonance frequency of the lower frequency hybrid mode. The opposite holds for the length of part B, d_{su}. The slot width H_{slot} influences the impedance matching, which is nearly unaffected by the slot length L_{slot}. Finally, the coaxial probe feed position (x_{coax} and y_{coax}) primarily determines the impedance matching, while also affecting the resonance frequencies of the hybrid modes. Similar to microstrip patch antennas with a finite groundplane [9], there is a length L_{gp} that maximizes the FTBR. A clear drawback of the half-mode implementation is loss of linear polarization. Yet, some degree of linear polarization remains. Therefore, the YZ-plane is referred to as the E-plane, and the XZ-plane as the H-plane.

The cavity width W_c is set to $27.5\,\text{mm}$, providing sufficient impedance bandwidth to meet the specifications. The length of the non-resonant slot L_{slot} equals $23.5\,\text{mm}$. The other antenna dimensions, being cavity lengths (d_{sl} and d_{su}), slot width (H_{slot}) and coaxial feed position (x_{coax} and y_{coax}), are optimized using CST Microwave Studio to meet the requirements. A groundplane length of $L_{gp} = 15.0\,\text{mm}$ achieves a FTBR of $13.9\,\text{dB}$, averaged over the $5\,\text{GHz}$ Wi-Fi band (Fig. 2). The resulting dimensions are annotated in Fig. 1b. Fig. 3 shows the simulated antenna reflection coefficient for average cork substrate ($\epsilon_r = 1.22$, $\tan\delta = 0.0363$), low-ϵ_r ($\epsilon_r = 1.17$, $\tan\delta = 0.0244$) and high-ϵ_r cork substrate ($\epsilon_r = 1.26$, $\tan\delta = 0.0421$), proving that the $5\,\text{GHz}$ Wi-Fi band remains covered for all cork substrates. For the average cork, the two hybrid modes resonate at $5.26\,\text{GHz}$ and $5.85\,\text{GHz}$, with mode profiles shown in Figs. 4a and 4b, respectively.

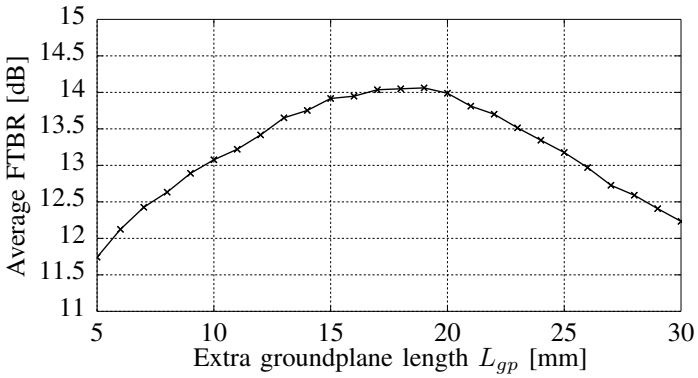

Fig. 2: Simulated front-to-back ratio [dB], as a function of extra groundplane length L_{gp}, averaged over the 5 GHz Wi-Fi band (5.15 GHz–5.85 GHz).

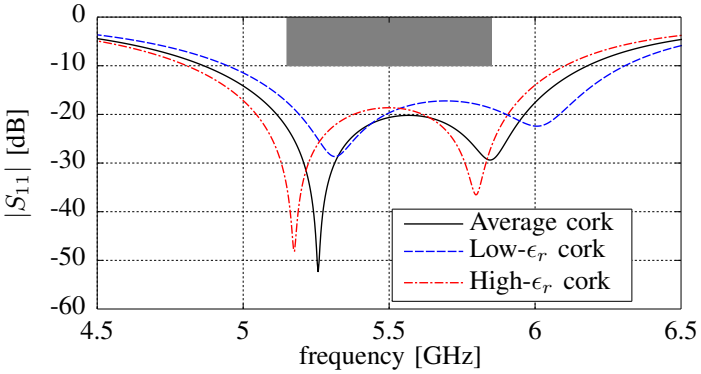

Fig. 3: Simulated reflection coefficient $|S_{11}|$ [dB] versus frequency, for different substrate parameters: average cork ($\epsilon_r = 1.22$, $\tan\delta = 0.0363$), low-ϵ_r cork ($\epsilon_r = 1.17$, $\tan\delta = 0.0244$) and high-ϵ_r cork ($\epsilon_r = 1.26$, $\tan\delta = 0.0421$).

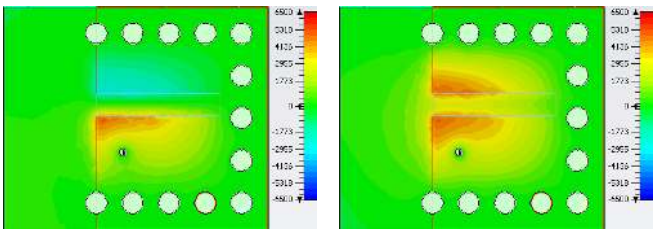

(a) strong TE_{120} + weak TE_{110} (b) strong TE_{110} + weak TE_{120}

Fig. 4: Simulated half-mode hybrid mode profiles: z-component of the electric field [V/m] at (a) 5.26 GHz and (b) 5.85 GHz.

III. Measurement Results

Anechoic chamber measurements, using an Agilent N5242A PNA-X Microwave Network Analyzer and an Orbit/FR DBDR antenna positioning system, validate the antenna performance in various operating conditions. Far-field radiation patterns are measured by the gain comparison method using a standard gain horn model MI-12-3.9. Table I summarizes the results.

Fig. 5 shows the simulated and measured input reflection

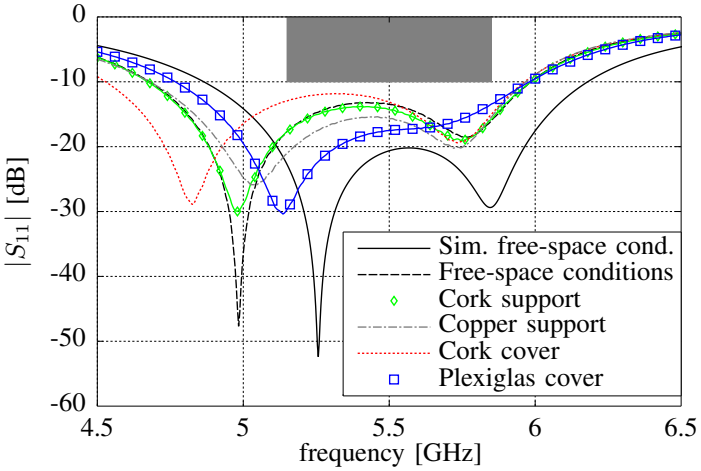

Fig. 5: Reflection coefficient $|S_{11}|$ [dB] versus frequency. Simulation in free-space conditions and measurements: free-space conditions, cork support, copper support, cork superstrate and Plexiglas superstrate.

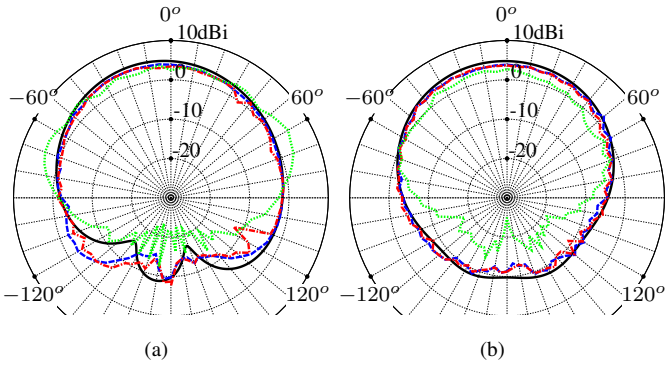

Fig. 6: Far-field gain pattern [dBi] in (a) the E-plane and (b) the H-plane at 5.50 GHz; simulation in free-space conditions (—) and measurements: free-space conditions (– – –), cork support (– · –) and copper support (· · ·).

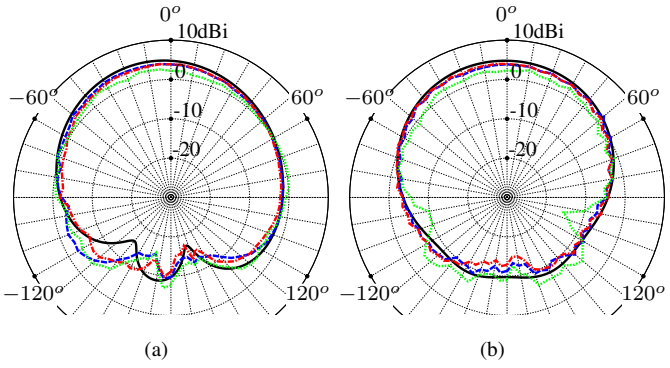

Fig. 7: Far-field gain pattern [dBi] in (a) the E-plane and (b) the H-plane at 5.50 GHz; simulation in free-space conditions (—) and measurements: free-space conditions (– – –), cork superstrate (– · –) and Plexiglas superstrate (· · ·).

TABLE I: Measured (simulated) antenna characteristics at 5.50 GHz for the different configurations

Configuration	radiation efficiency [%]	FTBR [dB]	maximum gain [dBi]
Free-space conditions	85 (83)	15.0 (14.5)	4.3 (5.0)
Cork support	79 (81)	14.8 (14.5)	4.1 (4.9)
Copper sheet support	84 (82)	27.4 (9.5)	4.9 (7.1)
Cork superstrate	80 (75)	16.8 (14.3)	4.2 (4.6)
Plexiglas superstrate	73 (—)	11.6 (—)	3.3 (—)

coefficients in free-space conditions. The antenna's impedance bandwidth of 1.30 GHz covers the entire 5 GHz Wi-Fi band. The slight difference between simulation and measurement is due to variations in the cork's dielectric properties and to fabrication inaccuracies, especially the feed probe's position. The simulated and measured far-field gain patterns in the E-plane and H-plane are shown in Fig. 6a and Fig. 6b, respectively. The measured maximum gain of 4.3 dBi, gain pattern shape, FTBR of 15.0 dB and radiation efficiency of 85 %, excellently agree with the simulation.

To confirm stable performance in different environments, the antenna's characteristics are also measured in the presence of dielectric or conducting platforms supporting the antenna, as well as various dielectric superstrates covering the antenna. When supporting the antenna by a 30 cm × 30 cm sheet of 3 mm thick cork, identical to the substrate material, almost no influence on the impedance matching (Fig. 5) or the gain pattern (Figs. 6a and 6b) is observed. The measured maximum gain of 4.1 dBi and FTBR of 14.8 dB are nearly identical to the results in free-space. A slightly lower radiation efficiency of 79 % is obtained, due to the additional losses in the cork support.

A 35 cm × 35 cm copper sheet support also leaves the impedance bandwidth (Fig. 5) practically unchanged. In contrast, the far-field gain pattern (Figs. 6a and 6b) is altered due to reflection on the copper surface. Figs. 6a and 6b demonstrate that back-radiation is significantly reduced and an improved FTBR of 27.4 dB is measured. No considerable decrease in radiation efficiency (84 %) is measured.

When covering the antenna by the aforementioned cork sheet, the impedance bandwidth (Fig. 5) significantly rises to 1.43 GHz, owing to a larger separation between the resonance frequencies of the two hybrid modes. The frequency band of interest remains covered. The far-field gain pattern (Figs. 7a and 7b) is slightly changed by the low ϵ_r superstrate. Both the measured maximum gain of 4.2 dBi and FTBR of 16.8 dB are not significantly modified compared to the undisturbed antenna. Additional losses in the cork superstrate only slightly reduce the measured radiation efficiency to 80 %.

Finally, we cover the antenna by a 30 cm × 30 cm sheet of 2.90 mm thick Plexiglas, with a spacing of 2 cm between the antenna and the Plexiglas. The impedance bandwidth (Fig. 5) reduces to 1.21 GHz, but the frequency band of interest remains covered. The Plexiglas, having a higher dielectric constant (typically 3.6), also clearly influences the radiation pattern (Figs. 7a and 7b). A reduced maximum gain of 3.3 dBi and a reduced FTBR of 11.6 dB are measured. A lower radiation efficiency of 73 % is obtained, due to additional losses in the Plexiglas.

The performed measurements show that only superstrates that cover the radiating slot have a slight influence on the impedance bandwidth of the antenna, either increasing or decreasing the impedance bandwidth. In the latter case, detuning of the antenna is successfully avoided by the incorporated impedance bandwidth margins.

IV. Conclusion

SIW cavity-backed antenna topologies are promising candidates to address the design challenges posed by IoT applications. Their potential is shown by designing and validating a wideband half-mode SIW cavity-backed slot antenna on a cork substrate, covering the 5 GHz Wi-Fi band. Cork, being a common floor and wall material, enables direct integration into a floor or wall. By impedance bandwidth overspecification, the design is successfully made robust to the inhomogeneity of the electrical properties of cork and fabrication inaccuracies. Moreover, the antenna provides stable performance in different environments, when various sheets of dielectrics or conductors support or cover the antenna. The antenna's compactness, integrability and stable high performance in different operating conditions, make it an ideal candidate for IoT applications.

Acknowledgment

Part of the work was supported by the iMinds IoT research program.

References

[1] H. Sundmaeker, P. Guillemin, P. Friess, and S. Woelfflé, Eds., *Vision and Challenges for Realising the Internet of Things*. Luxembourg: Publications Office of the European Union, 2010.

[2] M. Bozzi, A. Georgiadis, and K. Wu, "Review of substrate-integrated waveguide circuits and antennas," *IET Microwaves, Antennas & Propagation*, vol. 5, no. 8, pp. 909–920, June 2011.

[3] G. Q. Luo, T. Y. Wang, and X. H. Zhang, "Review of Low Profile Substrate Integrated Waveguide Cavity Backed Antennas," *International Journal of Antennas and Propagation*, vol. 2013, p. 7. [Online]. Available: http://dx.doi.org/10.1155/2013/746920

[4] Federal Communications Commission, "Revision of Part 15 of the Commission's Rules to Permit Unlicensed National Information Infrastructure (U-NII) Devices in the 5 GHz Band, First Report and Order, ET Docket No. 13-49," released April 1, 2014.

[5] R. Goncalves, R. Magueta, P. Pinho, and N. Carvalho, "RFID passive tag antenna for cork bottle stopper," in *2014 IEEE Antennas and Propagation Society International Symposium (APSURSI)*, July 2014, pp. 1518–1519.

[6] R. Moro, S. Agneessens, H. Rogier, A. Dierck, and M. Bozzi, "Textile Microwave Components in Substrate Integrated Waveguide Technology," *IEEE Transactions on Microwave Theory and Techniques*, vol. 63, no. 2, pp. 422–432, February 2015.

[7] G. Q. Luo, Z. F. Hu, W. J. Li, X. H. Zhang, L. L. Sun, and J. F. Zheng, "Bandwidth-Enhanced Low-Profile Cavity-Backed Slot Antenna by Using Hybrid SIW Cavity Modes," *IEEE Transactions on Antennas and Propagation*, vol. 60, no. 4, pp. 1698–1704, April 2012.

[8] Q. Lai, C. Fumeaux, W. Hong, and R. Vahldieck, "Characterization of the Propagation Properties of the Half-Mode Substrate Integrated Waveguide," *IEEE Transactions on Microwave Theory and Techniques*, vol. 57, no. 8, pp. 1996–2004, August 2009.

[9] H.-M. Lee, "Effect of partial ground plane removal on the front-to-back ratio of a microstrip antenna," in *7th European Conference on Antennas and Propagation (EuCAP)*, April 2013, pp. 1204–1208.